Carbohydrate Polymers 77 (2009) 80–86

Contents lists available at ScienceDirect

Carbohydrate Polymers

journal homepage: www.elsevier.com/locate/carbpol

Injection molded thermoplastic starch/natural rubber/clay nanocomposites: Morphology and mechanical properties

M. Mondragón [a,*], E.M. Hernández [b], J.L. Rivera-Armenta [c], F.J. Rodríguez-González [d]

[a] Instituto Politécnico Nacional, ESIME-Azcapotzalco, Sección de Estudios de Posgrado e Investigación, Av. de las Granjas 682, Col. Sta. Catarina, 02250 México, D.F., Mexico
[b] Instituto Politécnico Nacional, CICATA-Altamira, km 14.5 Carr. Tampico-Puerto Industrial, 89600 Altamira, Tamps., Mexico
[c] Instituto Tecnológico de Cd. Madero, Av. 1o. de Mayo esq. Sor Juana Inés de la Cruz s/n, 89440 Cd. Madero, Tamps., Mexico
[d] Centro de Investigación en Química Aplicada (CIQA), Blvd. Enrique Reyna 140, 25100 Saltillo, Coah., Mexico

ARTICLE INFO

Article history:
Received 5 June 2008
Received in revised form 4 November 2008
Accepted 4 December 2008
Available online 24 December 2008

Keywords:
Injection molding
Morphology
Nanocomposites
Natural rubber
Thermoplastic starch

ABSTRACT

Unmodified and modified natural rubber latex (uNRL and mNRL) were used to prepare thermoplastic starch/natural rubber/montmorillonite type clay (TPS/NR/Na^+-MMT) nanocomposites by twin-screw extrusion. After being dried, the nanocomposites were injection molded to produce test specimens. Scanning electron micrographs of fractured samples revealed that chemical modification of NRL enhanced the interfacial adhesion between NR and TPS; improving their dispersion. X-ray diffraction (XRD) showed that the nanocomposites exhibited partially intercalated/exfoliated structures. Surprisingly, transmission electron microscopy (TEM) showed that clay nanoparticles were preferentially intercalated into the rubber phase. Elastic modulus and tensile strength of TPS/NR blends were dramatically improved from 1.5 to 43 MPa and from 0.03 to 1.5 MPa, respectively, as a result of rubber modification. Properties of blends were almost unaffected by the dispersion of the clay except for the TPS/mNR blend loading 2% MMT. This was attributed to the exfoliation of the MMT.

1. Introduction

Recently, thermoplastic starch (TPS)/clay nanocomposites have received much attention because by adding minimal concentrations of clay, decreased water permeability and superior thermal and mechanical properties has been achieved (Chen & Evans, 2005; Huang, Yu, & Ma, 2004; Park, Lee, Park, Cho, & Ha, 2003; Park et al., 2002; Wilhelm, Sierakowski, Souza, & Wypych, 2003a; Wilhelm, Sierakowski, Souza, & Wypych, 2003b). Natural montmorillinite (Na^+-MMT) has turn to be effective for thermoplastic starch reinforcement (Park et al., 2002). It is composed of aluminosilicate layers stacked one above the other, whose layer thickness is around 1 nm and aspect ratios range from 10 to 1000 (Brune & Bicerano, 2002). The behavior of the TPS/MMT nanocomposites has been related to the dispersion of the MMT in the TPS matrix; which lead to the formation of intercalated/exfoliated nanostructures (McGlashan & Halley, 2003; Mondragón, Mancilla, & Rodríguez-González, 2008; Park et al., 2003). On the other hand, thermoplastic starches have being successfully blended with other suitable polymers to improve their mechanical properties and to reduce the dependence of their behavior on water content (Carvalho, Job, Alves, Curvelo, & Gandini, 2003; McGlashan & Halley, 2003). One of these polymer is natural rubber (NR, cis-1,4-polyisoprene). The NR grafted with the hydrophilic poly dimethylaminoethyl methacrylate (DMAEMA) has proven to be an efficient compatibilizer to obtain blends of plasticized starch and natural rubber with useful properties (Rouilly, Rigal, & Gilbert, 2004). Although the performance of injection molded compounds based on thermoplastic starch has been documented, a fundamental understanding of the behavior of injected TPS/clay nanocomposites is still lacking (Abbès, Ayad, Prudhomme, & Onteniente, 1998; Averous, Fauconnier, Moro, & Fringant, 2000; Leonor, Ito, Onuma, Kanzaki, & Reis, 2003; Onteniente, Abbès, & Safa, 2000; Souza Rosa & Andrade, 2004). Therefore, the scope of this work is to examine the combined effects of clay (Na+-MMT) content and rubber modification on the morphology and mechanical properties of injection molded TPS/NR/Na^+-MMT nanocomposites.

2. Experimental

2.1. Materials

2.1.1. Nanocomposites

Commercial corn starch MAIZENA® from Unilever de México SA de CV (Tultitlán, Edo. de México, México) and natural rubber latex (with a solid content of 37 weight percent, wt.%, and stabilized with ammonia) from a local producer were used. Glycerol was obtained from Productos Químicos Monterrey SA de CV (Monterrey,

---

* Corresponding author. Tel.: +52 55 5729 6300x64514; fax: +52 55 5729 6300x64493.
E-mail address: mmondragon@ipn.mx (M. Mondragón).

0144-8617/$ - see front matter © 2008 Elsevier Ltd. All rights reserved.
doi:10.1016/j.carbpol.2008.12.008

NL, México) and natural montmorillonite, Cloisite® Na^+, from Southern Clay Products (Gonzalez, TX, USA). Stearic acid from Productos Químicos Monterrey SA de CV (Monterrey, NL, México) and oxidized PE homopolymer, A-C® 316, from Honeywell International Inc. (Morristown, NJ, USA) were used as lubricants during processing.

2.1.2. Grafting

Dimethylaminoethyl methacrylate (DMAEMA), cumene hydroperoxide (CHP), and tetraethylene pentamine (TEPA), all reagent grade chemicals from Sigma–Aldrich Co. (St. Louis, MO, USA) were used as received.

2.2. Grafting procedure for natural rubber latex

The grafting procedure of DMAEMA onto NR was performed as described by Lamb, Anstey, Fellows, Monteiro, & Gilbert, 2001. Natural rubber latex (324.32 g), DMAEMA (12.10 g), CHP (0.46 g), and 2.5 wt.% ammonia solution (154 g) were combined and agitated with a low shear impeller at approximately 100 rpm under a nitrogen atmosphere over a period of 1 h to allow the partitioning of CHP into the rubber particles. TEPA (0.62 g, as a 10 wt.% solution in H_2O) was then added for over 1 h, at 5 min intervals, to initiate polymerization. The system was cooled in an ice/water bath for the first 8 h of reaction before gradual warming to room temperature and allowed to continue reacting for 16 h to obtain the modified latex.

2.3. Preparation of nanocomposites

Powdery formulations were prepared by mixing 800 g of starch with 0, 2, 4, and 6 wt.% Na^+-MMT (relative to dry rubber + starch), in a turbo-mixer Henchel at 740 rpm. Liquid formulations were prepared by hand mixing glycerol (24 wt.% of glycerol to the starch, dry bases) with the unmodified or modified natural rubber latex (15 wt.% of solid content to starch + glycerol), in a beaker. To prepare nanocomposites, both formulations were extruded and pelletized in a 29.4/1 L/D co-rotating Werner & Pflelderer ZSK 30 twin-screw extruder at 400 rpm. The temperature profile used was 80, 100, 150, 150 and 150 °C, measured from the feed section to the die. Pellets were dried in an oven for 12 h at 50 °C, and then injection molded into ASTM D638-72 Type 1 specimens, using an injection molding machine from Funchun Shin Co. LTD (China), provided with four electrically heating zones maintained at 150 °C.

2.4. Characterization of nanocomposites

A JEOL JSM-6100 scanning electron microscope (SEM) was used to investigate the morphology of the nanocomposites. The injected specimens were frozen under liquid nitrogen and fractured before being coated with gold/palladium on a JEOL JFC-1100E ion sputter coater. SEM micrographs were obtained using 15 kV secondary electrons.

The dispersion of the nanoclay in the polymer blends was evaluated by XRD and TEM. Wide-angle-X-ray scattering (WAXS) patterns were measured in reflection using a Siemens 7KP2021 diffractometer, with Cu Kα radiation at 35 kV and 25 mA. The injected samples were scanned in step mode by 2°/min scan rate in the range $2\theta < 10°$. The interlayer distance, d, was calculated according to Bragg's equation, $\lambda = 2d\sin\theta$. Ultrathin sections (about 80 nm) were cut from the injected specimens and transmission electron microscopy (TEM) observations were achieved with a JEOL JEM-1010 operating at 60 kV.

Tensile properties were evaluated according to the ASTM D638 on a 4467 Instron testing machine at a crosshead speed of 50 mm/min. Five dumbbell specimens were conditioned at 30% and 60% relative humidity (RH) for 15 days before the measurements, whose results were averaged to obtain a mean value.

Injected specimens of the nanocomposites were conditioned during two weeks at 25 °C and 60 ± 5% RH, before being tested using a dual cantilever clamp on a TA Instruments DMA-2980 dynamic thermo mechanical analyzer. The measurements were performed at a frequency of 1 Hz over a temperature range from −100 to 200 °C, at a scanning rate of 5 °C/mm.

3. Results and discussion

3.1. Morphology of the nanocomposites

Fig. 1 shows the SEM micrograph of the fractured surface of the TPS/uNR/MMT nanocomposite (prepared with unmodified natural rubber latex, uNRL) loading 4 wt.% clay. It reveals that both TPS matrix (light-gray areas) and dispersed rubber phase (dark-gray areas) are clearly separated indicating lack of interfacial adhesion. This is expected because NR and TPS are immiscible due to the hydrophobic character of the former and the hydrophilic character of the latter (Rouilly et al., 2004). Although it has been reported that the proteins and lipids present at the surface of the rubber particles act as compatibilizers between starch and rubber molecules, these interactions are not strong enough to obtain a good dispersion in these blends (Carvalho et al., 2003).

On the other hand, the use of mNRL (Fig. 2a) resulted in a finer dispersion and improved interfacial adhesion. At higher magnification (Fig. 2b), it is seen that the TPS domains seem to be covered with a layer that looks like a fine mesh. It was supposed that the poly(DMAEMA)-grafted polyisoprene chains adhered to the starch phase are responsible for the formation of this layer. As reported by other authors, blending of TPS with modified polyisoprene leads to the formation of hydrogen bonds between latex particles with a "hairy layer" of surface-grafted hydrophilic poly(DMAEMA) and starch molecules (Kangwansupamonkon, Gilbert, & Kiatkamjornwong, 2005; Rouilly et al., 2004). The fibrils should have been formed by plastic deformation.

3.2. Na^+-MMT dispersion

Fig. 3 shows the diffraction patterns of pristine clay (MMT), TPS/uNR/MMT and TPS/mNR/MMT nanocomposites. The interlayer distance (d_{001}) = 1.15 nm of pristine clay (diffraction peak at

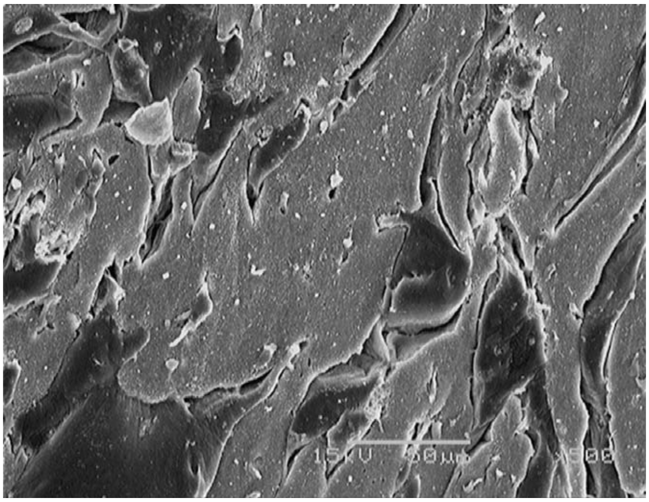

Fig. 1. SEM micrograph of the fractured TPS/uNR/Na^+-MMT nanocomposite containing 4 wt.% clay.

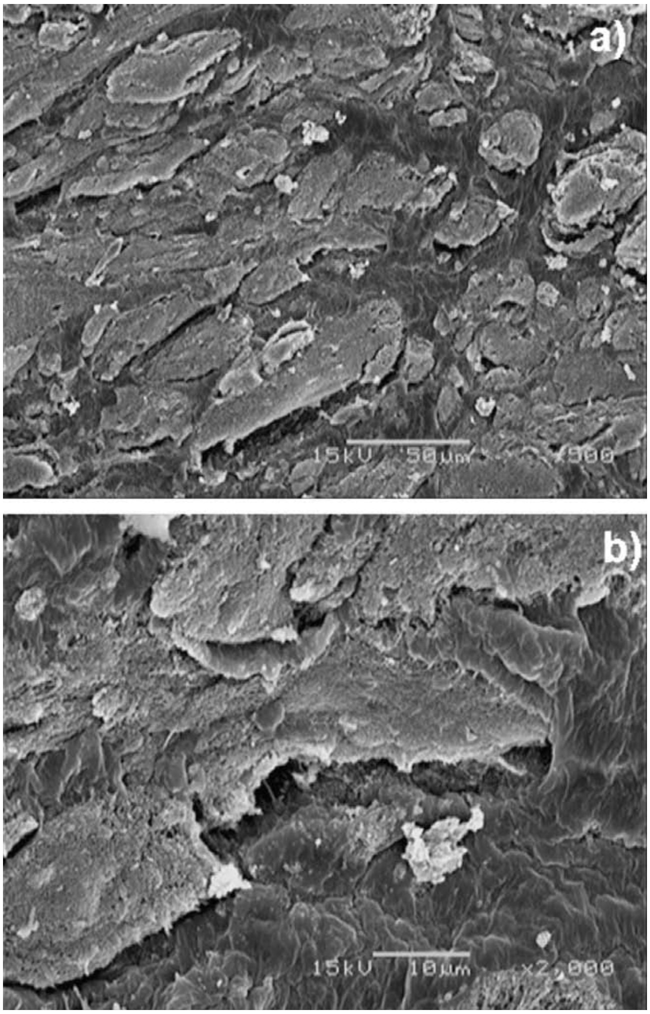

Fig. 2. SEM micrographs of the fractured TPS/mNR/Na$^+$-MMT nanocomposite containing 4 wt.% clay, at different magnifications.

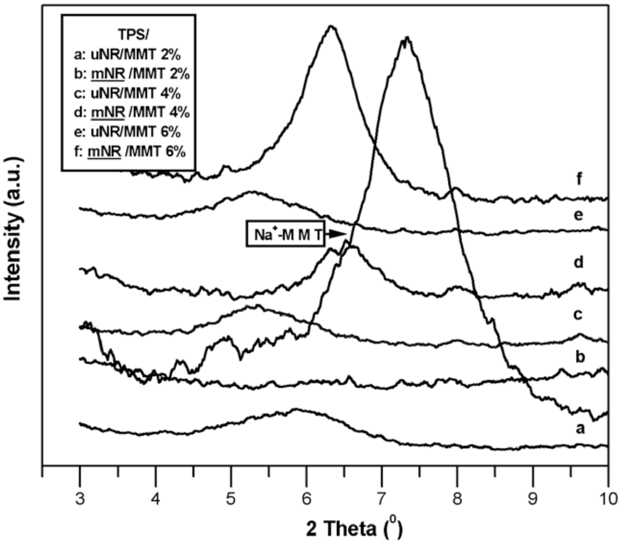

Fig. 3. Effect of Na$^+$-MMT content and chemical modification of NR on the XRD spectra of TPS/uNR/Na$^+$-MMT and TPS/mNR/Na$^+$-MMT nanocomposites.

$2\theta = 7.68°$), expanded to 1.51, 1.65 and 1.67 nm for the TPS/uNR/MMT nanocomposites loading 2, 4 and 6 wt.% MMT, respectively. For the TPS/mNR/MMT nanocomposites loading 4 and 6 wt.% MMT, the interlayer distance expanded to 1.36 and 1.39 nm, respectively. This behavior clearly indicates that for either type of nanocomposite, the polymer chains are intercalated into the silicate layers forming well-ordered intercalated structures. Surprisingly, TPS/mNR/MMT loading 2 wt.% clay showed no detectable peak, which can be assumed as evidence of exfoliated structures.

TEM images were used to confirm the dispersion of Na$^+$-MMT in the TPS/NR matrixes. Dispersion of clay has been reported in both TPS (Chen & Evans, 2005; Huang et al., 2004; Park et al., 2002, 2003; Wilhelm et al., 2003a, 2003b) and NR matrixes (Varghese & Karger-Kocsis, 2003). In the former, high polarity produced by hydroxyl groups of TPS matrix has been related to the intercalation of the layered silicates. On the other hand, clay dispersion in NR latex has been related to clay "swelling" into the aqueous medium. Fig. 4 displays the TEM images of TPS/uNR/MMT (Fig. 4a) and TPS/mNR/MMT (Fig. 4b) nanocomposites loading 4 wt.% MMT. White areas correspond to TPS matrix and dark areas to NR domains. It can be observed in both figures, that the Na$^+$-MMT is dispersed only in the NR domains forming well-ordered intercalated structures (see arrows). This is quite unexpected considering that starch has higher polarity than NR. Other authors have found similar clay-natural rubber compatibility (Valadares, Leite, & Galambeck, 2006).

Several factors could have contributed to the formation of these structures only in NR domains. High acting shear forces during melt compounding can cause the diffusion of polymer chains within the silicate galleries, especially for polymers of high molecular weight like the natural rubber (Varghese, Karger-Kocsis, & Gatos, 2003). Also, the polar groups of the proteins and lipids, at the surface of NR, may act as a driving force for rubber chains to intercalate into the silicate layers (Carvalho et al., 2003). Another factor for the presence of the silicates preferentially in the NR domains could be the ammonia used to stabilize the latex. Although the surface polarities of both clay and NR latex particles, are negative (Rippel, Leite, & Galembeck, 2002), the excess of ammonium cations on the surface of stabilized NR latex particles, contribute to match the polarities of the polymer and clay improving their compatibility via electrostatic interactions, which in turn favors intercalation. The layers of the Na$^+$-MMT are usually expanded or delaminated by exchanging Na$^+$ with alkylammonium cations therefore, it can be assumed that the ammonia greatly facilitate the intercalation of the polyisoprene chains (Chen, Teng, Tsai, & Yen, 2006).

3.3. Mechanical properties

Figs. 5–7 show the tensile properties of the TPS/NR/MMT nanocomposites conditioned at 30 and 60% RH. Tensile strength (σ) and elastic modulus (E) of TPS/uNR blend conditioned at 30% RH are 0.03 and 1.5 MPa, respectively (Figs. 5 and 6). The use of mNR resulted in a significant increment of both σ and E: tensile strength increased from 0.03 to 5 MPa and elastic modulus increased from 1.5 to 43 MPa. Meaning that σ was increased by 167% and E by 30% when compared to TPS/uNR. This significant increase could be attributed to the combination of enhanced compatibility between the modified NR and starch and the crosslinking of polyalkenylene chains (Lamb et al., 2001; Rouilly et al., 2004). Conditioning starch-based materials at high relative humidities (RH) would result in water absorption and, consequently, to a weakening effect of the water at the interface between the polymer matrix components and the silicate layers, as suggested for other fillers (Karger-Kocsis, 2000). σ of TPS/uNR and TPS/mNR blends decreased 50% when nanocomposites were conditioned at 60% RH, whereas E droped more than 75%. Dispersion of the MMT resulted in almost no change in the mechanical behavior of the blends; the

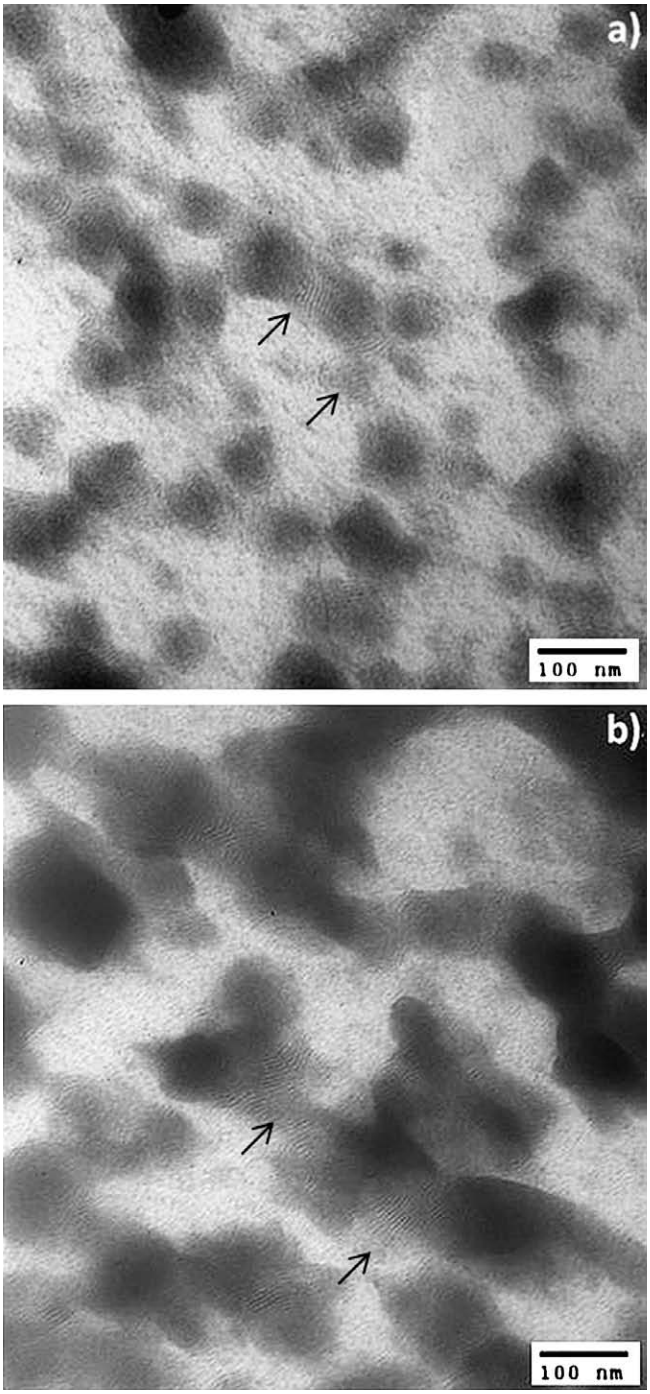

Fig. 4. TEM micrographs of: (a) TPS/uNR/Na$^+$-MMT and (b) TPS/mNR/Na$^+$-MMT nanocomposites containing 4 wt.% clay.

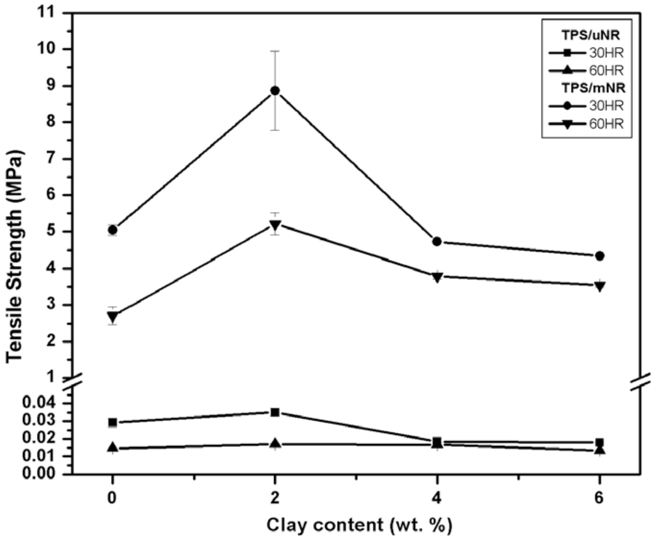

Fig. 5. Tensile strength (σ of TPS/uNR/Na$^+$-MMT and TPS/mNR/Na$^+$-MMT nanocomposites as a function of clay content and relative humidity (RH).

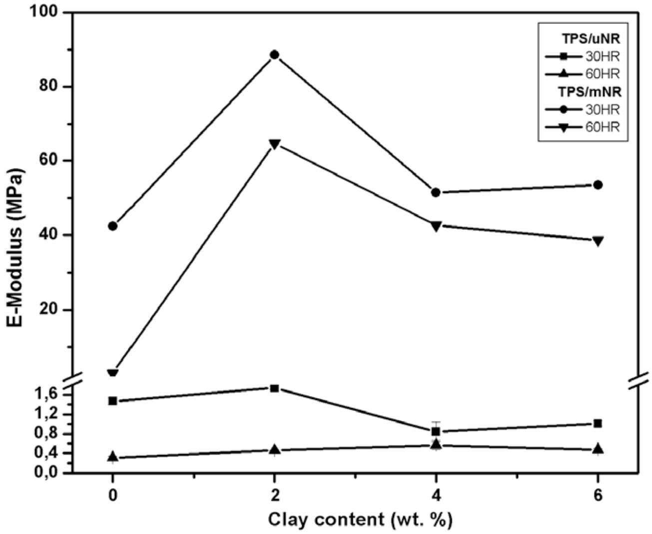

Fig. 6. *E*-modulus of TPS/uNR/Na$^+$-MMT and TPS/mNR/Na$^+$-MMT nanocomposites as a function of clay content and relative humidity (RH).

only exception was observed in the case of the TPS/mNR blend loading 2 wt.% MMT. XRD showed that clay in this nanocomposite was completely exfoliated (Fig. 3) and it is probable that some silicate layers were also present into TPS matrix. It has been reported that the mechanical properties of polymeric nanocomposites are improved when exfoliated structures are present since stresses are effectively transferred increasing the reinforcement effect (Jordan, Jacob, Tannenbaum, Sharif, & Jasiuk, 2005).

At 30% RH, TPS/uNR/MMT nanocomposites fail in fragile manner regardless of clay content (Fig. 7). In the same way, TPS/mNR/MMT nanocomposites remained fragile independently of clay content and RH. Low elongation of the TPS/mNR/MMT nanocomposites could be attributed to partial crosslinking of polyalkenylene chains. Conversely, elongation at break of TPS/uNR/MMT nanocomposites conditioned at 60% RH was 65% for TPS/uNR blend having 0 wt.% clay and this value tended to decrease as clay content increased. Ductility of TPS/uNR/MMT at 60% RH is typical of a plasticized polymer system, charged with a rigid particulate filler (Wilhelm et al., 2003a).

3.4. Dynamic mechanical analysis

The thermomechanical properties of the TPS/NR/Na$^+$-MMT nanocomposites were evaluated in order to verify the influence of clay content and functionalization of the NR.

The storage modulus (G') and the mechanical loss factor ($\tan\delta$) of the TPS/uNR/MMT nanocomposites as a function of temperature are shown in Fig. 8. A major transition detectable about −40 °C, which onset temperature was around −60 °C, was noticed. The glass transitions (T_g) of polymers can be related to the onset of the pronounced decreased in the elastic modulus (Wielage,

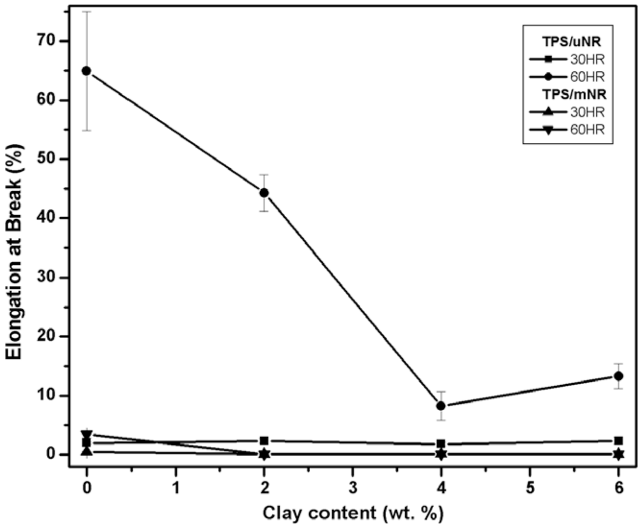

Fig. 7. Elongation at break of the TPS/uNR/Na^+-MMT and TPS/mNR/Na^+-MMT nanocomposites as a function of clay content and relative humidity (RH).

Lampke, Utschik, & Soergel, 2003). The T_g of the polyisoprene is at −63 °C (Angellier, Molina-Boisseau, & Dufresne, 2005). On the other hand, several authors have reported two thermal transitions for TPS materials: one below room temperature (from −74 and −54 °C) associated to a glycerol-rich phase and the second in the range from 20 to 150 °C, associated to a starch-rich phase. The values of these transitions vary depending on water and glycerol content (Averous & Boquillon, 2004; Rodriguez-Gonzalez, Ramsay, & Favis, 2004; Wilhelm et al., 2003a). Hence, the modulus drop at −40 °C could correspond to both rubber and glycerol-rich phase relaxations. Below this transition, values of G' increased as clay content increased indicating that MMT affects the elastic properties associated to the rubber phase. As shown in TEM micrographs (Fig. 4), silicate layers are mainly dispersed into NR domains. By contrast, G' decreased at high temperatures compared to the unfilled TPS/uNR blend.

The tan δ peak of the unfilled TPS/uNR blend was also increased upon the addition of 4 and 6 wt.% clay Fig. 4b. Higher clay loading produces more tactoids leading to lower interfacial adhesion (McGlashan & Halley, 2003). The relaxation associated to the starch-rich phase was also seen in the plot of tan δ. The increment of the broad shoulder of the TPS/uNR blends loading 4% and 6% clay may be attributed to moisture loss and releasing of the interlayer water molecules of the clay (Chiou, Yee, Glenn, & Orts, 2005; Wilhelm et al., 2003a).

The storage modulus (G') of TPS/mNR/MMT nanocomposites presented more important increasing at all the investigated temperature range, compared to TPS/uNR/MMT nanocomposites, due to mNR crosslinking and improved adhesion of TPS/mNR interface, as observed in Fig. 9a (Rouilly et al., 2004; Lamb et al., 2001).

Unexpectedly, analysis of tan δ of TPS/mNR/MMT nanocomposites revealed that thermal transition at −40 °C does not change netiher by the influence of clay content nor by rubber crosslinking (Fig. 9b). On the other hand, the relaxation associated to the starch-rich phase become sharper and more intense with a maximum ca. 60, 80, 90 and 90 °C for the TPS/mNR/MMT nanocomposites with 0, 2%, 4% and 6% MMT content, respectively. This can be explained by greater changes in the moisture loss and the releasing of the interlayer water molecules of the clay due to the presence of the hydrophilic poly(DMAEMA), as well as to the interactions between the starch and the grafted and ungrafted poly(DMAEMA) (Rouilly et al., 2004; Wilhelm et al., 2003a).

4. Conclusions

TPS/uNR/Na^+-MMT and TPS/mNR/Na^+-MMT nanocomposites were prepared by melt mixing in a co-rotating twin-screw extruder and then injection molded. The influence of clay content and rubber modification on the morphology and mechanical properties of the injected nanocomposites were studied. As expected, the chemical modification of NR improved both the dispersion and interfacial adhesion of the rubber phase in the TPS matrix. This

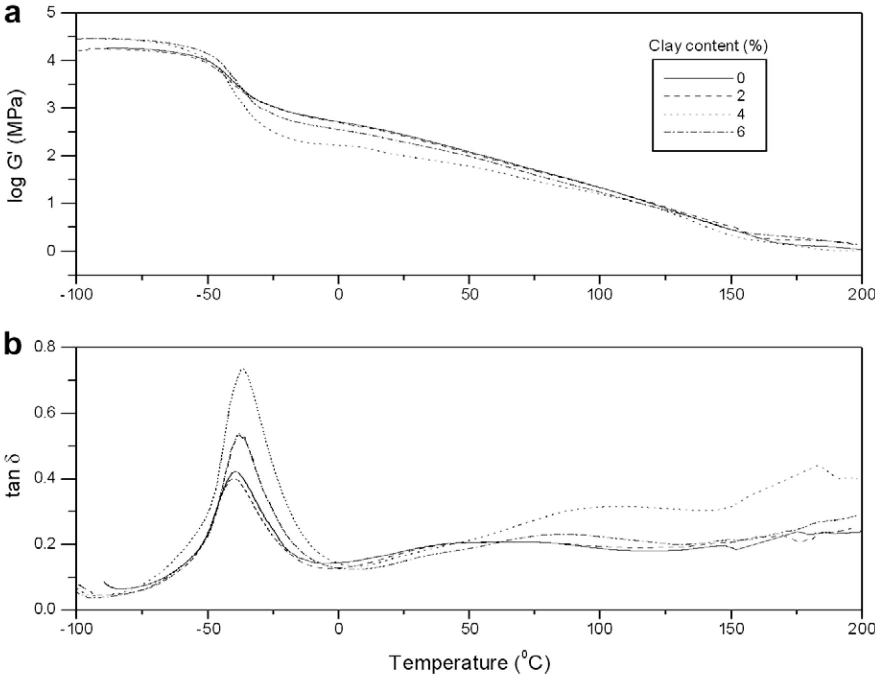

Fig. 8. (a) Storage modulus (G') and (b) mechanical loss factor (tan δ) (b) of TPS/uNR/Na^+-MMT nanocomposites, as a function of clay content.

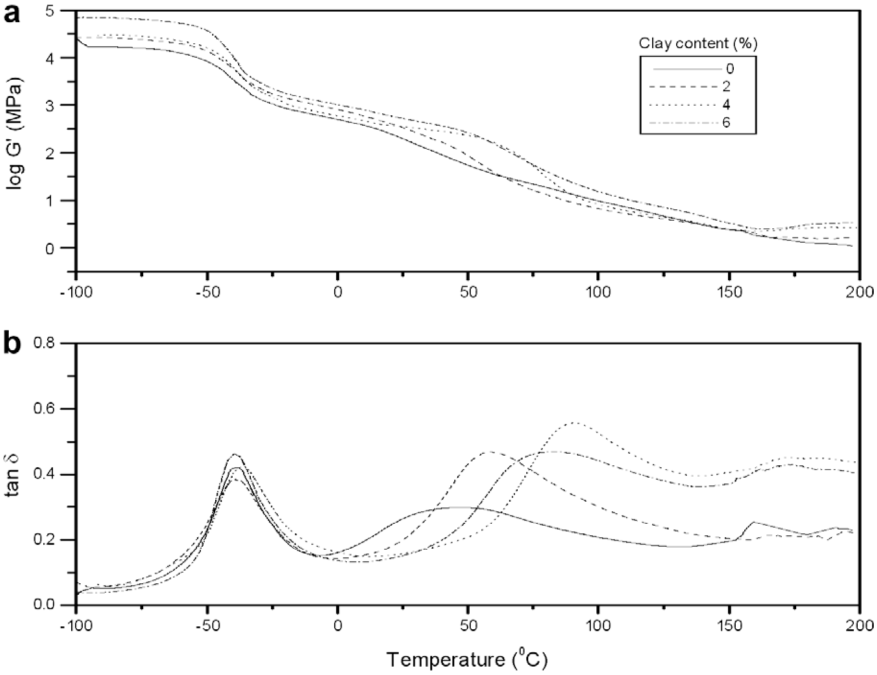

Fig. 9. (a) Storage modulus (G') and mechanical loss factor (tan δ) (b) of TPS/mNR/Na$^+$-MMT nanocomposites, as a function of clay content.

improvement combined with the NR crosslinking occurring during chemical modification, resulted in very significant increase of tensile strength and elastic modulus as compared to TPS/uNR blends. Addition of 2 wt.% MMT led to exfoliated structures which further increased the tensile properties of the TPS/mNR blend, demonstrating the benefits of using both modified rubber molecules and nanoclay particles. Surprisingly, nanoclay particles were mainly dispersed in the NR domains. This was explained by excess of ammonia cations which contributed to improve the interfacial compatibility between rubber and clay particles via electrostatic interactions.

Acknowledgments

Financial support from CONACYT-SAGARPA (project 11893) is acknowledged. The authors would like to thank to M.E Sánchez (ENCB-IPN), and J.G. Rodriguez, M. Palacios and F. Zendejo (CIQA) for technical assistance.

References

Abbès, B., Ayad, R., Prudhomme, J.-C., & Onteniente, J.-P. (1998). Numerical simulation of thermoplastic wheat starch injection molding process. *Polymer Engineering and Science, 38*, 2029–2038.

Angellier, H., Molina-Boisseau, S., & Dufresne, A. (2005). Mechanical properties of waxy maize starch nanocrystal reinforced natural rubber. *Macromolecules, 38*, 9161–9170.

Averous, L., & Boquillon, N. (2004). Biocomposites based on plasticized starch: thermal and mechanical behaviors. *Carbohydrate Polymers, 56*, 111–122.

Averous, L., Fauconnier, N., Moro, L., & Fringant, C. (2000). Blends of thermoplastic starch and polyesteramide: processing and properties. *Journal of Applied Polymer Science, 76*, 1117–1128.

Brune, D. A., & Bicerano, J. (2002). Micromechanics of nanocomposites : comparison of tensile and compressive elastic moduli, and prediction of effects of incomplete exfoliation and imperfect alignment on modulus. *Polymer, 43*, 369–387.

Carvalho, A. J. F., Job, A. E., Alves, N., Curvelo, A. A. S., & Gandini, A. (2003). Thermoplastic starc/natural rubber blends. *Carbohydrate Polymers, 53*, 95–99.

Chen, B., & Evans, J. R. G. (2005). Thermoplastic starch–clay nanocomposites and their characteristics. *Carbohydrate Polymers, 61*, 455–463.

Chen, C. H., Teng, C. C., Tsai, M. S., & Yen, F. S. (2006). Preparation and characterization of rigid poly(vinyl chloride)/MMT nanocomposites. II. XRD, morphological and mechanical characteristics. *Journal of Polymer Science Part B: Polymer Physics, 44*, 2145–2154.

Chiou, B. S., Yee, E., Glenn, G. M., & Orts, W. J. (2005). Rheology of starch–clay nanocomposites. *Carbohydrate Polymers, 59*, 467–475.

Huang, M. F., Yu, J. G., & Ma, X. F. (2004). Studies on the properties of montmorillonite-reinforced thermoplastic starch composites. *Polymer, 45*, 7017–7023.

Jordan, J., Jacob, K. I., Tannenbaum, R., Sharif, M. A., & Jasiuk, I. (2005). Experimental trends in polymer nanocomposites – a review. *Material Science and Engineering A, 393*, 1–11.

Kangwansupamonkon, W., Gilbert, R. G., & Kiatkamjornwong, S. (2005). Modification of natural rubber by grafting with hydrophilic vinyl monomers. *Macromolecular Chemistry and Physics, 206*, 2450–2460.

Karger-Kocsis, J. (2000). Reinforced polymer blends. In D. R. Paul & C. B. Bucknall (Eds.). *Polymer blends* (Vol. 2, pp. 411–413). New York: John Wiley and Sons, Inc..

Lamb, D. J., Anstey, J. F., Fellows, C. M., Monteiro, M. J., & Gilbert, R. G. (2001). Modification of natural and artificial polymer colloids by "topology-controlled" emulsion polymerization. *Biomacromolecules, 2*, 518–525.

Leonor, I. B., Ito, A., Onuma, K., Kanzaki, N., & Reis, R. L. (2003). In vitro bioactivity of starch thermoplastic/hydroxyapatite composite biomaterials: an in situ study using atomic force microscopy. *Biomaterials, 24*, 579–585.

McGlashan, S., & Halley, P. J. (2003). Preparation and characterization of biodegradable starch-based nanocomposite materials. *Polymer International, 52*, 1767–1773.

Mondragón, M., Mancilla, J. E., & Rodríguez-González, F. J. (2008). Nanocomposites from plasticized high-amylopectin, normal and high-amylose maize starches. *Polymer Engineering and Science, 48*, 1261–1267.

Onteniente, J.-P., Abbès, B., & Safa, L. H. (2000). Fully biodegradable lubricated thermoplastic wheat starch: mechanical and rheological properties of an injection grade. *Starch, 52*, 112–117.

Park, H. M., Lee, W. K., Park, C. Y., Cho, W. J., & Ha, C. S. (2003). Environmentally friendly polymer hybrids. *Journal of Materials Science, 38*, 909–915.

Park, H. M., Li, X., Jin, C. Z., Park, C. Y., Cho, W. J., & Ha, C. S. (2002). Preparation and properties of biodegradable thermoplastic starch/clay hybrids. *Macromolercular Materials and Engineering, 287*, 553–558.

Rippel, M. M., Leite, C. A. P., & Galembeck, F. (2002). Elemental mapping in natural rubber latex films by electron energy loss spectroscopy associated with transmission electron microscopy. *Analytical Chemistry, 74*, 2541–2546.

Rodriguez-Gonzalez, F. J., Ramsay, B. A., & Favis, B. D. (2004). Rheological and thermal properties of thermoplastic starch with high glycerol content. *Carbohydrate Polymers, 58*, 139–147.

Rouilly, A., Rigal, L., & Gilbert, R. G. (2004). Synthesis and properties of composites of starch and chemically modified natural rubber. *Polymer, 45*, 7813–7820.

Souza Rosa, R. C. R., & Andrade, C. T. (2004). Effect of chitin addition on injection-molded thermoplastic corn starch. *Journal of Applied Polymer Science, 92*, 2706–2713.

Valadares, L. F., Leite, C. A. P., & Galambeck, F. (2006). Preparation of natural rubber-montmorillonite nanocomposite in aqueous medium: evidence for polymer-platelet adhesion. *Polymer, 47*, 672–678.

Varghese, S., & Karger-Kocsis, J. (2003). Natural rubber-based nanocomposites by latex compounding with layered silicates. *Polymer, 44*, 4921–4927.

Varghese, S., Karger-Kocsis, J., & Gatos, K. G. (2003). Melt compounded epoxidized natural rubber/layered silicate nanocomposites: structure-properties relationships. *Polymer, 44*, 3977–3983.

Wielage, B., Th, Lampke, Utschik, H., & Soergel, F. (2003). Processing of natural-fibre reinforced polymers and the resulting dynamic-mechanical properties. *Journal of Materials Processing Technology, 139*, 140–146.

Wilhelm, H. M., Sierakowski, M. R., Souza, G. P., & Wypych, F. (2003a). Starch films reinforced with mineral clay. *Carbohydrate Polymers, 52*, 101–110.

Wilhelm, H. M., Sierakowski, N. R., Souza, G. P., & Wypych, F. (2003b). The influence of layered compounds on the properties of starch/layered compound composites. *Polymer International, 52*, 1035–1044.